Core chirality based tailoring of the liquid crystalline properties of supermolecular tetrapedes†

Abdelhak Belaissaoui, Stephen J. Cowling, Isabel M. Saez and John W. Goodby*

Received 22nd December 2009, Accepted 24th February 2010
First published as an Advance Article on the web 25th March 2010
DOI: 10.1039/b927008f

A series of novel supermolecular star-shaped tetrapede chiral liquid crystals (LCs), incorporating carbohydrates, methyl α-D-glucopyranoside or methyl α-D-mannopyranoside, as chiral cores surrounded by four cyanobiphenyl mesogenic groups linked by either C6 or C11 alkyl chain spacers, have been synthesised. These non-conventional thermotropic carbohydrate-based chiral liquid crystals exhibit chiral nematic and smectic A mesophases over broad temperature ranges. The mesomorphic properties were characterized by polarized optical microscopy (POM) and differential scanning calorimetry (DSC). The effect of the flexible spacer length in addition to the stereogenic and conformational properties of the chiral cores is discussed.

1. Introduction

One of the most fascinating and challenging fields in material science is the design and development of novel materials, endowing predictable or desirable functionalities and physical properties.

As a consequence of the self-assembling properties of liquid crystals and their self-organized dynamic structures, the control and fine-tuning of their mesomorphic and physical properties can be achieved by structural engineering at the molecular level.

In recent years, the design and functionalisation of supermolecular liquid crystals (Fig. 1) have been the subject of growing and intense interest as a result of their molecular architectures,[1] which combine the self-organizing properties of low molecular weight LCs and the ability to form secondary or tertiary conformational structures of polymeric-like liquid crystals.[2] Furthermore, they provide the possibility of incorporating specific functionalities with precise nature and location, allowing the elaboration of highly functional materials with unique tailored properties. Hence, the molecular engineering approach to highly structured materials leads to further understanding of self-assembling and self-organizing processes and subsequently fine-tuning control of mesophase formations.

There are various factors influencing the mesomorphic behaviour of supermolecular liquid crystals and are particularly based on: (i) the degree of flexibility/rigidity, dimensional properties (linear, planar or three dimensional) and structural/chemical nature (stereogenic properties, hydrophobic, hydrophilic, aromatic,…) of the inner scaffold; (ii) the length of the spacer, which controls the degree of decoupling of the mesogens from the core; (iii) the nature and density of the mesogenic units at the periphery, as well as the topology of the attachments to the core (end-on and side-on).

Thereby, the liquid crystalline properties are related to the overall molecular topology in relation to the inner core (Fig. 2), aspect ratios, conformational dynamics,[3] dipolar properties and specific inter- and intra-molecular interactions. Moreover, at the macroscopic level, nanosegregation of building blocks and their space filling efficiency in condensed phase are two competing driving forces for the molecular self-assembly in liquid-crystalline phases.[4]

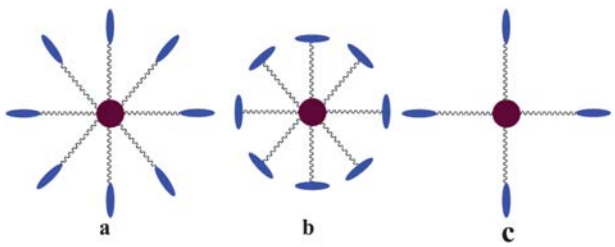

Fig. 1 Primary structures of polypedal supermolecules with mesogens as (a) end-on (b) side-on (c) tetramer supermolecule with end-on mesogenic groups.

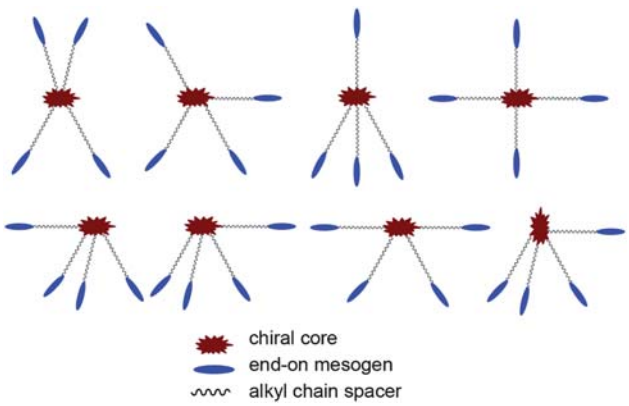

Fig. 2 Schematic representations of primary structures of molecular tetrapedes displaying the orientational effect of the tetravalent chiral core on the overall shape anisometry.

Department of Chemistry, University of York, York, YO10 5DD, UK. E-mail: jwg500@york.ac.uk

† Electronic supplementary information (ESI) available: Experimental procedures, POM micrographs and MALDI-TOF. See DOI: 10.1039/b927008f

Our aim, in an approach to chiral dendritic supermolecular LCs,[1] is to modify their functional behaviour and investigate the manifestation of the stereogenic structural properties on their mesomorphic behaviour. This can be achieved by incorporating chirality within the dendritic structure, as multivalent core and branching points, which can affect the microenvironment of the dendrimer and ultimately their mesomorphic properties.

Carbohydrates represent a large class of liquid crystals that form thermotropic as well as lyotropic mesophases.[5] The driving force for the mesomorphic behaviour in amphiphilic carbohydrate derivatives is the microphase segregation. Hence, chiral thermotropic mesophases are not observed in amphiphilic carbohydrate liquid crystals, despite their chiral nature and optical activity. Surprisingly, there have been very few reports on the synthesis and mesomorphic properties of supermolecular liquid crystals with carbohydrates as chiral cores and mesogenic units attached at the periphery.[6]

The profound importance of carbohydrates in molecular recognition processes,[7] combined with their structurally and stereochemically diverse commercial availability, makes them particularly attractive as a promising source for novel liquid crystalline materials. In this context, we incorporated enantiomerically pure carbohydrate derived units, as cores for the synthesis of chiral dendritic supermolecules.

In this paper, we report the synthesis of supermolecular chiral liquid crystals incorporating either methyl α-D-glucopyranoside or methyl α-D-mannopyranoside as the chiral cores surrounded by four cyanobiphenyl mesogenic groups linked by a spacer either penta- or deca-methylene carboxylate units (Scheme 1). The two carbohydrate cores differ only at the C2 position with the R configuration for the methyl α-D-glucoside and S for the methyl α-D-mannoside. We demonstrate the effect of the stereogenic and associated conformational properties of the core and the length of the flexible spacer on the liquid crystalline properties.

2. Results and discussions

2.1. Synthesis

Two conceptually different synthetic strategies, summarised in Fig. 3, can be applied for the preparation of the tetramer supermolecules **G*n*** and **M*n*** (n = 1 and 2). The divergent approach, corresponding to the synthetic strategy A, consists of assembling stepwise the branched tetramer from the core to the periphery. In the first step, the four spacers are attached to the core, followed by tetrafold coupling of the end-on pro-mesogenic groups. In contrast, in the convergent synthetic approach B, the arms consisting of the mesogen and alkyl spacer are prepared initially before their attachment to the core.

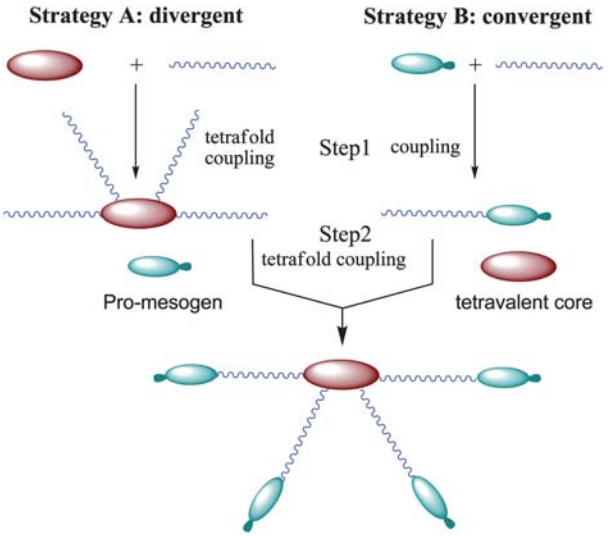

Fig. 3 Conceptual synthetic strategies applied for the synthesis of tetramer supermolecules **G*n*** and **M*n*** (n = 1 and 2).

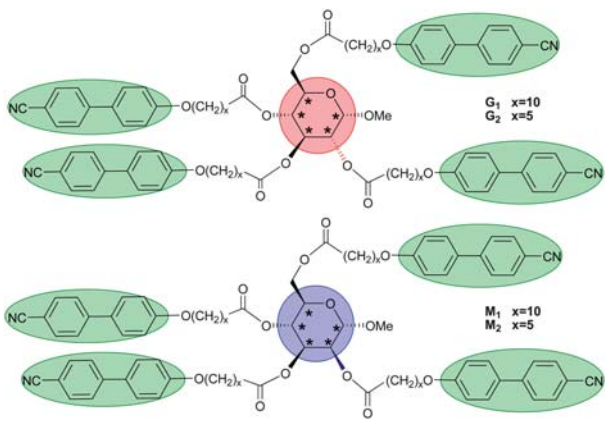

Scheme 1 Molecular structures of the chiral supermolecular carbohydrate-based liquid crystal tetramers.

The synthesis of tetramers **G*n*** and **M*n*** (n = 1 and 2) is outlined in Scheme 2. 11-(4-Cyanobiphenyl-4′-yloxy)undecanoic acid **3a** and 6-(4-cyanobiphenyl-4′-yloxy)hexanoic acid **3b** were obtained in excellent yield by the oxidation of the corresponding alcohols 11-(4-cyanobiphenyl-4′-yloxy)undecanol **2a** and 6-(4-cyanobiphenyl-4′-yloxy)hexanol **2b** with Jones reagent in acetone.

The esterification reactions of methyl α-D-glucopyranoside and methyl α-D-mannopyranoside with the carboxylic acids **3a** and **3b** in CH_2Cl_2 using DCC as coupling reagent in the presence of a catalytic amount of DMAP, afforded the corresponding tetramers **G*n*** and **M*n*** (n = 1 and 2) in quantitative yields and as monodisperse structures. The reactions were monitored by GPC to completion for two weeks. The slow kinetic rate is most likely owing to the low solubility of the carboxylic acids and their corresponding intermediates in CH_2Cl_2.

Alternatively, the carboxylic acids **3a** and **3b** were synthesised following synthetic route 2 (Scheme 2), by etherification reaction of ethyl-11-bromo-undecanoate and ethyl-6-bromo-hexanoate with 4-cyano-4′-hydroxybiphenyl **1**, followed by hydrolysis reaction in KOH ethanolic solution.[8] However, the coupling of the resulting carboxylic acids **3a** and **3b** with methyl α-D-glucopyranoside and methyl α-D-mannopyranoside yielded the tetramers **G*n*** and **M*n*** (n = 1 and 2) as polydisperse materials. Evidence from ^{1}H NMR showed a residual downfield proton signal at 8.05 ppm, assigned to two aromatic protons adjacent to an amide group. In addition, two highfield residual resonances, a triplet at 1.4 ppm and a quadruplet at 4.4 ppm, were recorded and assigned to ethyl ester group.

As suggested by ^{1}H NMR investigation, the observed distribution can be rationalised by the partial coupling of the

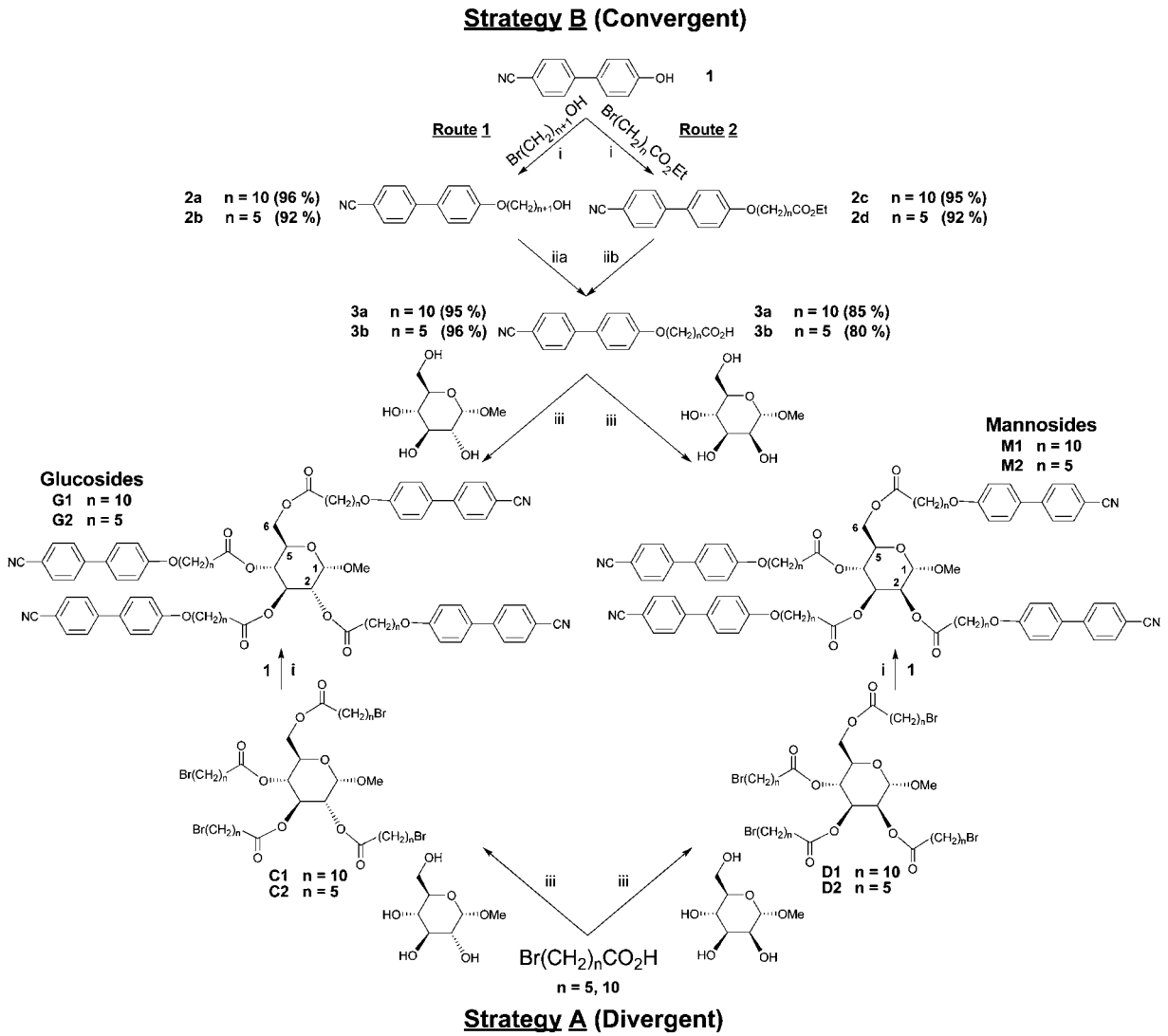

Scheme 2 *Reagents and conditions*: (i) K_2CO_3/KI, butanone, (iia) Jones reagent, acetone, (iib) KOH/EtOH, (iii) DCC/CH_2Cl_2.

glucoside and mannoside cores with ethyl-11-(4-carbamoylbiphenyl-4′-yloxy)undecanoate and ethyl-6-(4-carbamoylbiphenyl-4′-yloxy)hexanoate, present in slight amount in the reaction mixture. The amide derivatives are byproducts obtained in very low yields, resulting from the partial hydrolysis of cyano groups under strong basic conditions to amide moieties, during the hydrolysis reactions of the esters **2c** and **2d** (Scheme 2).

Moreover, the divergent synthetic strategy A (Fig. 3) has been attempted (Scheme 2). Esterification reactions of 11-bromo-undecanoic acid and 6-bromo-hexanoic acid with methyl α-D-glucopyranoside and methyl α-D-mannopyranoside using DCC as coupling reagent in CH_2Cl_2 yielded the tetrabromo-tetramers **C*n*** and **D*n*** ($n = 1$ and 2), followed by etherification reactions with the 4-cyano-4′-hydroxybiphenyl **1** to obtain the tetramers **G*n*** and **M*n*** ($n = 1$ and 2). However, the esterification reactions of the glucoside and mannoside cores with 11-bromo-undecanoic acid and 6-bromo-hexanoic acid did not progress to completion and as a consequence the purification of the branched tetramers proved to be difficult. Furthermore, the monodispersity of **G*n*** and **M*n*** might be hardly controllable from the etherification reactions of **C*n*** and **D*n*** with 4-cyano-4′-hydroxybiphenyl.

These results suggest that the optimal synthetic approach to obtain **G*n*** and **M*n***, as supermolecular monodisperse structures, can be achieved by using the convergent synthetic strategy B (Fig. 3) with the arms prepared *via* synthetic route 1 (Scheme 2), involving the etherification reaction using mild deprotonating agent K_2CO_3 and the consecutive oxidation with chromic acid.

2.2. Mesomorphic properties

The mesomorphic properties of the synthesised compounds were investigated by polarized optical microscopy (POM) and differential scanning calorimetry (DSC).

The optical defect textures of the tetramers **G1** and **M1**, consisting of long alkyl spacer C11 and either methyl α-D-glucoside or methyl α-D-mannoside cores respectively, exhibit enantiotropic SmA mesophases with typical fan-shaped textures.

The DSC traces of **G1** and **M1** were recorded, during the third heating and cooling run, at a scanning rate of 10 °C min^{-1}. On the heating run of **G1** (Fig. 4), the first endothermic transition at lower temperature region corresponds to the glassy state obtained at midpoint 21.0 °C and a second endothermic

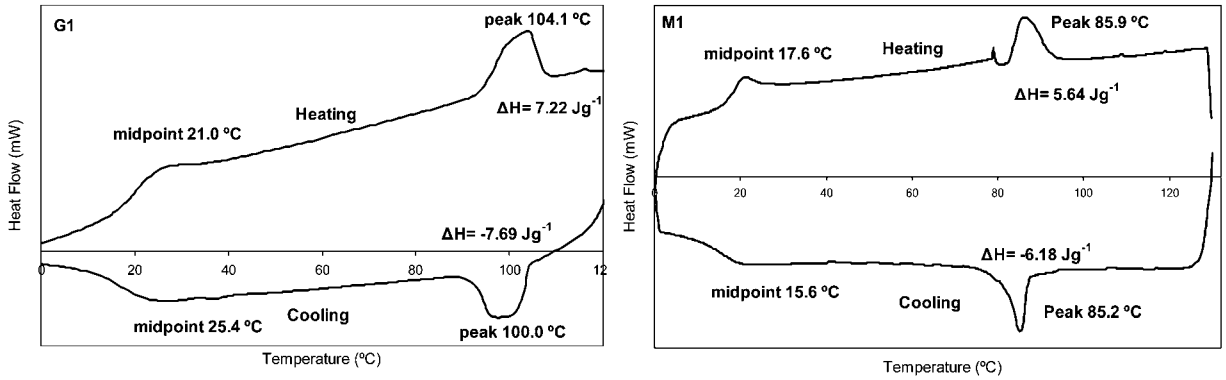

Fig. 4 DSC thermograms of star-shaped liquid crystals **G1** and **M1**.

Table 1 Phase transition temperatures (°C) and corresponding enthalpy values (J g^{-1})

Gluco-tetrapedes	Manno-tetrapedes
G1 Iso 100.9 ($\Delta H = -7.69$) SmA 25.4 T_g	**M1** Iso 87.2 ($\Delta H = -6.18$) SmA 15.6 T_g
G2 Iso 112.0 ($\Delta H = -1.15$) N* 41.9 T_g	**M2** Iso 84.4 ($\Delta H = -1.44$) N* 35.2 T_g

transition with peak signal at 104.1 °C ($\Delta H = 7.22$ J g^{-1}). Upon cooling, two exothermic transitions were observed, the first peak at 100 °C ($\Delta H = -7.69$ J g^{-1}) and a broad glassy transition at midpoint 25.4 °C. The measured thermal properties are summarised in Table 1.

The ability of pyranose monosaccharides to access more than one low energy conformation, as a consequence of their conformationally dynamic nature (Fig. 5), clearly has an effect on their phase behaviour in the condensed phase.

This is the case when comparing compounds **G1** and **M1**, which differ only in configuration at the stereogenic centre C2, corresponding to R and S respectively. The increased ordering for the glucoside tetramer is seemingly owing to specific spatial conformation of the arms in relation to the chiral core (Fig. 6), revealing an expression of the chirality[9] at macromolecular level in thermotropic mesophases. This is remarkable, as the spacer length C11 is sufficiently long that one would expect that the mesogens would be highly decoupled from the core.[10] Macroscopically, the SmA mesophase formation for **G1** and **M1** can be rationalized by the high flexibility of the cyanobiphenyl mesogenic arms, as a consequence of the conformationally dynamic cores (Fig. 5 and 6), but mainly owing to the long alkyl chain spacer, allowing the most stable arrangements of the mesogen units in their dipole-driven anti-parallel correlations.[11]

Similarly, the defect textures of the compounds **G2** and **M2** were investigated by thermal polarized optical microscopy. After slow cooling from isotropic state and annealing, **G2** exhibits a fine-grain texture while **M2** displays a poorly defined granular texture. Evidences from POM suggest right handed helical ordering for **G2** and **M2**, thereby indicating chiral nematic mesophases.

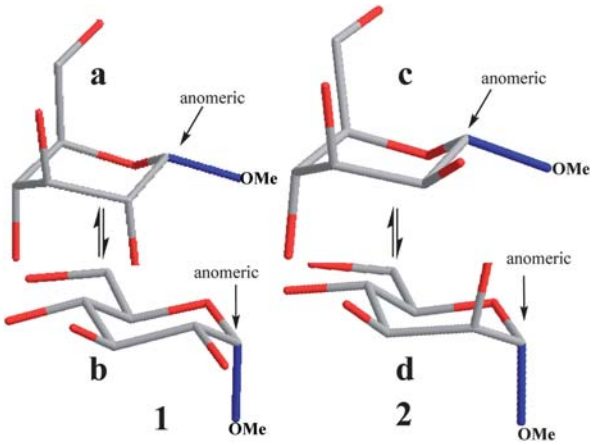

Fig. 5 Conformational diversity associated with glucoside and mannoside confers high versatility and flexibility to the chiral cores (arms are hidden for clarity). Glucoside chair conformations (**1**) with four arms in **a**, all in axial positions, and **b**, all in equatorial positions. Mannoside chair conformations (**2**) with four arms in **c**, three axial and one equatorial, and **d**, three equatorial and one axial.

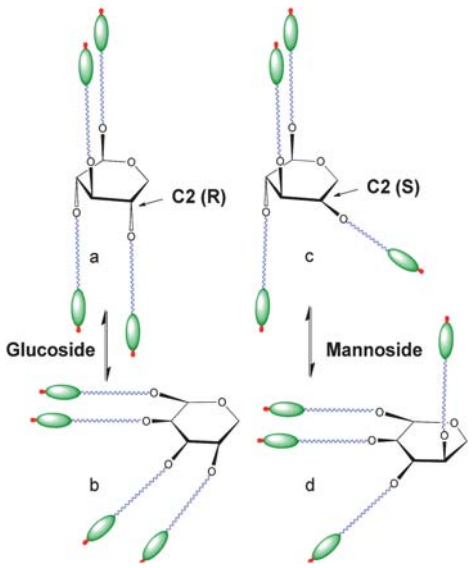

Fig. 6 Topological orientations of the four arms in the two chair conformations associated with **G*n*** (a and b) and **M*n*** (c and d) ($n = 1$ and 2) incorporating glucoside and mannoside inner cores, respectively. Groups are hidden for clarity.

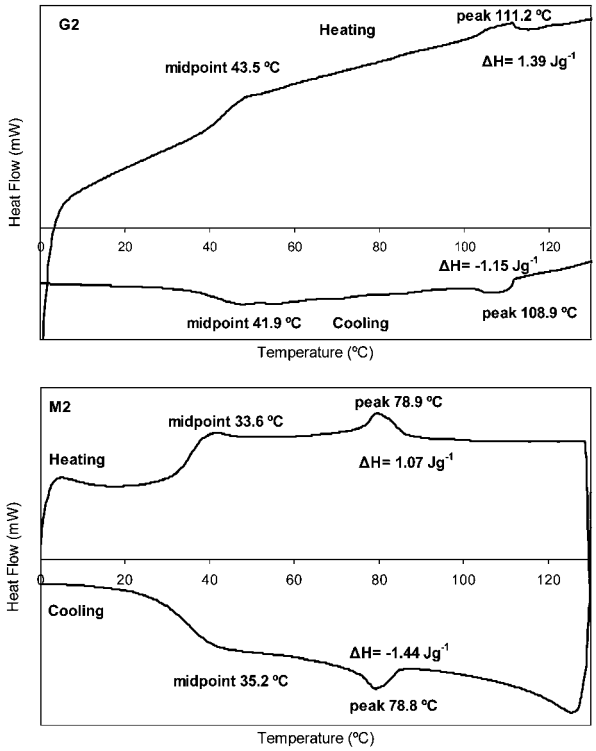

Fig. 7 DSC thermograms of star-shaped liquid crystals **G2** and **M2**.

Phase transition behaviours of **G2** and **M2** were analysed by DSC. The thermograms are shown in Fig. 7 and the transition temperatures are listed in Table 1. Both materials, which are in the glassy state at room temperature, undergo enantiotropic transitions during the DSC analysis.

On the heating cycle of **G2**, the endothermic glassy broad transition occurred at midpoint 43.5 °C, which was followed by a second transition with a peak signal at 111.2 °C ($\Delta H = 1.39$ J g^{-1}) marking the transition from chiral nematic to isotropic phase.

The cooling cycle showed a first exotherm with its peak at 108.9 °C ($\Delta H = -1.15$ J g^{-1}), associated with the isotropic–chiral nematic transition. Further cooling induced a broad glassy transition at midpoint 41.9 °C.

Interestingly, tetrapedes **G*n*** and **M*n*** ($n = 1$ and 2) displayed relatively broad DSC signals corresponding to anisotropic–isotropic transitions. This can be attributed to the gradual conformational changes affecting the packing properties of the glucoside and mannoside bulks during their corresponding anisotropic–isotropic transitions.

It is noteworthy that, in comparison with **G1** and **M1**, both **G2** and **M2** presented broader DSC signals and extremely low enthalpy values for the anisotropic–isotropic transitions on cooling and heating cycles, indicating relatively disordered mesophases. In addition, on cooling **G2** rapidly developed a grainy texture associated with a right-handed helicity suggesting a chiral nematic mesophase, while **M2** showed similar phase ordering and handness with a relatively poorly defined texture.

On the other hand, **G1** and **M1** displayed higher enthalpy values for the anisotropic–isotropic phase transitions on cooling and heating, reflecting an enhanced mesogenic ordering (SmA) in comparison to **G2** and **M2**. In addition, **G1/G2** gave rise to, in comparison to **M1/M2**, relatively wider mesophase temperature ranges, respectively.

Comparison of the transition temperatures reveals a decrease in the isotropisation temperature from the glucosides **G*n*** ($n = 1$ and 2) to mannosides **M*n*** ($n = 1$ and 2), thereby indicating lower thermal stability of the mannoside mesophases.

The clearing-point temperature depression upon changing the chiral core structure from glucoside to mannoside can be attributed to the orientational and conformational properties associated with each inner chiral core (Fig. 5 and 6), influencing the thermal stability and dictating the phase behaviour.

When attaching long spacer C11, glycoside and mannoside tetramers **G1** and **M1** display wide temperature range SmA mesophases. In contrast, incorporating a shorter spacer C6 induces right-handed chiral nematic mesophases associated with an increase in the glassy temperature transition, regardless of the chiral core structure.

The molecular modelling geometries of the optimized **G*n*** and **M*n*** ($n = 1$ and 2) molecules in gas phase using the molecular mechanics 2 (MM2) force fields, shown in Fig. 8, reveal large free volume between the four individual arms.

For all the models, the MeO groups attached to the anomeric carbons C1 are in axial positions. The core conformation with the lowest steric energy in **G*n*** ($n = 1$ and 2), corresponds to the model with all four arm substituents in equatorial positions (Fig. 6b). On the other hand, for the mannoside derivatives **M*n*** ($n = 1$ and 2), it is attributed to 3,4,5-triequatorial with an axial arm substituent at C2 position (Fig. 6d).

In the condensed state, any voids have to be compensated for.[4] This can be achieved by internal folding and/or hosting. Since star-shaped structures **G*n*** and **M*n*** present large internal molecular free volume in single molecule state, modelling their supramolecular organisation into mesophases would be challenging, due the structural complexity and conformational diversity.

There are various elements of structural flexibility within the tetramers: conformationally dynamic cores, the alkyl chain spacers and the four connecting ester groups.

Due to the higher flexibility of the alkyl chain spacers C11, the tendency of **G1** and **M1** to efficiently fill space in liquid crystal

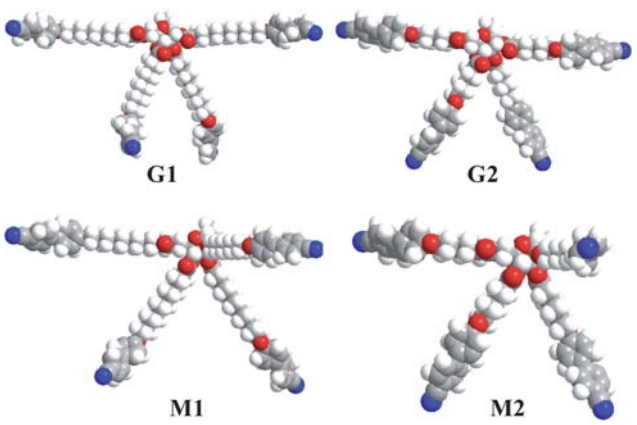

Fig. 8 Side-on view 3D space-filling models of **G*n*** and **M*n*** ($n = 1$ and 2) tetramer conformers after energy minimisation at 0 K in gas phase using the molecular mechanics 2 (MM2).

state would be higher in comparison with **G2** and **M2** bearing shorter spacers C6.

The conformational molecular sketches **a** and **c** (Fig. 6), corresponding alternatively to glucoside and mannoside cores, reveal fewer voids than their corresponding counterparts **b** and **d**, and thus space filling effects would favour the first two conformations.

Comparing the nanoscale self-organizing properties of **G2** and **M2**, the space filling efficiency effect is the predominant factor in rationalizing their different thermal and mesomorphic properties.

3. Conclusions

A novel series of tetrapodal star-shaped carbohydrate-based chiral liquid crystals have been synthesised. The inner cores consist of glucoside or mannoside derivatives, which can acquire several flexible conformations. The effect of the flexible spacer length on the liquid crystalline property was investigated.

G1 and **M1**, incorporating long spacer C11, display wide temperature range SmA mesophases. In the case of **G2** and **M2**, bearing shorter arms C6, the tetramers exhibit chiral nematic self-ordering, associated with an increase in the glassy temperature transitions, independently of the chiral core structure. Furthermore, upon changing the chiral core structure from glucoside to mannoside, clearing-point temperature depression was observed, regardless of the length of the spacer.

In summary, the fine-tuning of the mesomorphic properties of the tetramer polypedes **G*n*** and **M*n*** can be achieved depending on carbohydrate-based conformationally dynamic chiral core structure and the spacer length, controlling the degree of the decoupling between the core and the cyanobiphenyls. Therefore, tailoring the thermo-mesomorphic behaviour of the supermolecular tetrapedes **G*n*** and **M*n*** can be achieved by combining the core chirality and spacer length.

Acknowledgements

This work has been financed by EPSRC Grant EP/E064299/1 within the EUROCORES Programme SONS II of the European Science Foundation. We also thank the EPSRC Mass Spectrometry Service at Swansea for MALDI-TOF MS analyses.

Notes and references

1 J. W. Goodby, I. M. Saez, S. J. Cowling, V. Görtz, M. Draper, A. W. Hall, S. Sia, G. Cosquer and E. P. Raynes, *Angew. Chem., Int. Ed.*, 2008, **47**, 2754–2787; I. M. Saez and J. W. Goodby, *Struct. Bonding*, 2008, **128**, 1–62; B. Donnio, S. w. Buathong, I. Bury and D. Guillon, *Chem. Soc. Rev.*, 2007, **36**, 1495–1513; C. T. Imrie and P. A. Henderson, *Chem. Soc. Rev.*, 2007, **36**, 2096–2124.

2 *Handbook of Liquid Crystals. Vol. 3: High Molecular Weight Liquid Crystals*, ed. D. Demus, J. W. Goodby, G. W. Gray, H.-W. Spiess and V. Vill, Wiley-VCH, Weinheim, 1998, ISBN 3-527-29272-1.

3 R. Kannan, T. Sen, R. Poupko, Z. Luz and H. Zimmerman, *J. Phys. Chem. B*, 2003, **107**, 13033; H. Zimmermann, V. Bader, R. Poupko, E. J. Wachtel and Z. Luz, *J. Am. Chem. Soc.*, 2002, **124**, 15286–15301; M. Lehmann, M. Jahr, B. Donnio, R. Graf, S. Gemming and I. Popov, *Chem.–Eur. J.*, 2008, **14**, 3562–3576.

4 C. Tschierske, *Chem. Soc. Rev.*, 2007, **36**, 1930; M. Lehmann, M. Jahr, F. C. Grozema, R. D. Abellon, L. D. A. Siebbeles and M. Muller, *Adv. Mater.*, 2008, **20**, 4414–4418; R. Mezzenga, J. Ruokolainen, N. Canilho, E. Kasëmi, D. A. Schlüter, W. B. Lee and G. H. Fredrickson, *Soft Matter*, 2009, **5**, 92–97.

5 J. W. Goodby, V. Gortz, S. J. Cowling, G. Mackenzie, P. Martin, D. Plusquellec, T. Benvegnu, P. Boullanger, D. Lafont, Y. Queneau, S. Chambert and J. Fitremann, *Chem. Soc. Rev.*, 2007, **36**, 1971–2032, and references within C. M. Paleos, *Mol. Cryst. Liq. Cryst.*, 1994, **243**, 159–183; C. Tschierske, *Prog. Polym. Sci.*, 1996, **21**, 775–852; G. A. Jeffrey and L. M. Wingert, *Liq. Cryst.*, 1992, **12**, 179–202; H. Prade, R. Miethchen and V. Vill, *J. Prakt. Chem./Chem.-Ztg.*, 1995, **337**, 427–440.

6 M. Tian, B. Y. Zhang, Y. H. Cong, N. Zhang and D. S. Yao, *J. Mol. Struct.*, 2009, **923**(1–3), 39–44; H. Akiyama, A. Tanaka, H. Hiramatsu, J. Nagasawa and N. Tamaoki, *J. Mater. Chem.*, 2009, **19**, 5956–5963; B. Zhang, W. Xiao, Y. Cong and Y. Zhang, *Liq. Cryst.*, 2007, **34**(10), 1129–1136; W. Q. Xiao, B. Y. Zhang and Y. H. Cong, *Chem. Lett.*, 2007, 938–939.

7 P. Sears and C. H. Wong, *Proc. Natl. Acad. Sci. U. S. A.*, 1996, **93**, 12086–12093; *Encyclopedia of supramolecular chemistry*, ed. J. L. Atwood and J. W. Steed, Taylor & Francis Ltd, London, 2004, A. Lützen, pp. 169–177, ISBN: 0824747232 A.

8 R. Lunkwitz, C. Tschierske and S. Diele, *J. Mater. Chem.*, 1997, **7**(10), 2001–2012; Y. Xia, R. Verduzco, R. H. Grubbs and J. A. Kornfield, *J. Am. Chem. Soc.*, 2008, **130**(5), 1735–1740.

9 Themed issue: Nanoscale chirality, *Chem. Soc. Rev.*, 2009, (3); *Materials-Chirality (Topics in Stereochemistry Vol. 24)*, ed. M. M. Green, R. J. M. Nolte and E. W. Meijer, John Wiley & Sons, Hoboken, New Jersey, 2003, ISBN: 9780471054979, Online ISBN: 9780471471899.

10 H. Finkelmann, M. Happ, M. Portugal and H. Ringsdorf, *Makromol. Chem.*, 1978, **179**, 2541–2544.

11 D. P. E. Smith, H. Hörber, C. Gerber and G. Binnig, *Science*, 1989, **245**, 43–45; D. P. E. Smith and W. H. Heckl, *Nature*, 1990, **346**, 616–617; D. P. E. Smith, J. K. H. Hörber, G. Binnig and H. Nejoh, *Nature*, 1990, **344**, 641–644; S. Taki, T. Kadotani and S. Kai, *J. Phys. Soc. Jpn.*, 1999, **68**(4), 1286–1291.